Research Square

Preprints are preliminary reports that have not undergone peer review.
They should not be considered conclusive, used to inform clinical practice,
or referenced by the media as validated information.

A Novel 1D Helical Coordination Polymer Based on Cu2+ /L-Arginine-Schiff Base: Structure and Supramolecular Insights

Syed Meheboob Elahi

meheboob.elahi@gmail.com

Maulana Abul Kalam Azad University of Technology, West Bengal

Research Article

Keywords: Coordination Polymer, Amino acid-Schiff base, Hirshfeld Surface Analyses

Posted Date: May 15th, 2026

DOI: https://doi.org/10.21203/rs.3.rs-9597683/v1

License: This work is licensed under a Creative Commons Attribution 4.0 International License.
Read Full License

Additional Declarations: No competing interests reported.

Version of Record: A version of this preprint was published at Transition Metal Chemistry on August 26th, 2026. See the published version at https://doi.org/10.1007/s11243-026-00766-7.

A Novel 1D Helical Coordination Polymer Based on Cu^{2+}/L-Arginine-Schiff Base: Structure and Supramolecular Insights

Dr. Syed meheboob Elahi*[a]
Department of Applied Science and Humanities
Bengal Institute of Technology and Management, Santiniketan
Dwaranda, BYPASS P.O, Sriniketan, West Bengal 731236
meheboob.elahi@gmail.com
Orcid ID: 0000-0002-7418-2770

Abstract: A chiral one-dimensional (1D) helical coordination polymer, $[Cu(SalArgH)]NO_3 \cdot H_2O$ (referred to as CuAr), has been synthesized using an L-arginine-derived Schiff base ligand ($SalArgH_2$) and characterized by single-crystal X-ray diffraction. The Cu(II) center shows a distorted square pyramidal geometry, with the tridentate ligand bridging adjacent metal ions to form an extended polymeric chain. The inherent chirality of the L-arginine moiety guides the formation of a helical structure, effectively transferring molecular chirality into the extended coordination framework. Hirshfeld surface analysis reveals that the crystal packing and stabilization of the helical structure are primarily influenced by O···H hydrogen bonds, with significant contributions also coming from C···H and N···H contacts. Electronic absorption studies reveal transitions such as $\pi \rightarrow \pi^*$, $n \rightarrow \pi^*$, ligand-to-metal charge transfer, and weak d–d transitions, which are affected by ligand field effects and Jahn–Teller distortion. Circular dichroism (CD) spectroscopy provides insights into the development of chiral coordination polymers derived from amino acids.

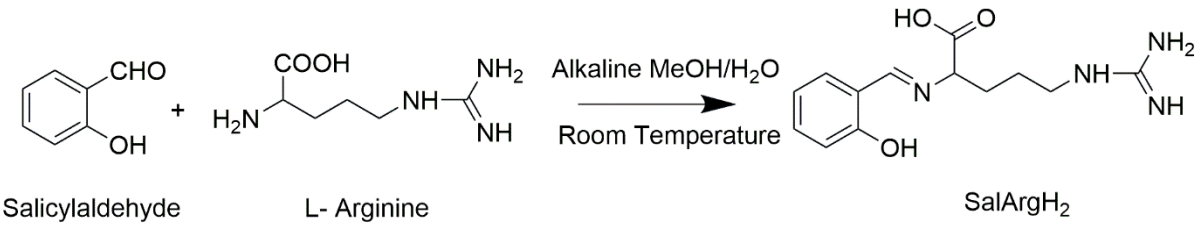
.

Keywords: Coordination Polymer; Amino acid-Schiff base; ; Hirshfeld Surface Analyses

Introduction

Over the past few decades, significant progress has been made in understanding the chemistry of transition metal complexes with amino acid-Schiff base ligands.[1] Most studies on these metal complexes have focused on the different binding modes of these ligands. X-ray crystal structures of such complexes have shown that Schiff base ligands primarily act as a tridentate moiety, coordinating through the phenolate oxygen, imine nitrogen, and carboxylate oxygen. Additionally, several reports have demonstrated their biological importance, including antimicrobial activity,[2] anticancer effects,[3] antioxidant properties,[4] and others. L-arginine is an essential amino acid and is generally safe to use as a supplement.[5] It can effectively lower blood pressure and address other health issues in humans. From a coordination chemistry perspective, L-arginine is a chiral ligand that can bind to metal ions via both its amine and carboxylic groups [6], and it may also have microbiological activity. Numerous L-arginine-derived Schiff base systems, especially those made from salicylaldehyde, have been widely studied for their various biofunctional properties, including DNA binding and cleavage[7], photonuclease activity,[8] and photocytotoxic effects.[3] Structural analyses based on single-crystal X-ray diffraction show that these systems mainly form mononuclear, discrete metal complexes, where the Schiff base ligand stabilizes the metal center through tridentate coordination.[7-8]

Herein, we used $SalArgH_2$(Scheme 1.)[9], a Schiff base, followed by a complexation with Cu^{2+}, resulting in a 1D coordination polymer that is chiral and forms a helical structure due to a long side chain originating from the amino acid (i.e., L-arginine). Notably, coordination polymers exclusively based on Schiff base ligands are relatively less explored compared to discrete complexes, although some examples have been reported in recent years.[10-13] To the best of our knowledge, this work represented the first coordination polymer based on $SalArgH_2$. Hirshfeld surface (HS) analysis was employed to gain a deeper understanding of the packing and vital interactions [14] that guide the supramolecular arrangement in the crystalline state of the 1D coordination polymer. Moreover, electronic spectra, including circular dichroism (CD), also revealed the chiral helical nature of this 1D coordination polymer.



Scheme 1. Representation of ligand $SalArgH_2$ preparation methodology.

Experimental

Materials and Physical Measurements

All chemicals were reagent grade and obtained from commercial sources and used without purification. The solvents were purified by standard procedures. Infrared spectra were measured on a Perkin-Elmer FT-IR spectrometer with KBr pellets in the range of 4000–450 cm^{-1} (Fig. in ESI S1 & S2 for ligand and complex, respectively). Elemental analysis was carried out in a PerkinElmer 2500 series II elemental analyzer. PXRD data were collected on Bruker D8 Advance and matched with a simulated pattern (Fig. SI 3). UV–vis spectra were recorded on an Agilent Technologies Cary 60 UV-Vis.

Synthesis of Ligand $SalArgH_2$

In a 100 ml methanolic solution of the salicylic acid (0.5 ml, ~5.0mmol), 50 ml alkaline aqueous-methanolic solution of L-arginine was added (0.870g, 5.0 mmol) and stirred in cold conditions for 30 min, and the resulting yellow colored solution was kept for slow evaporation at room temperature. Within two days, a yellow-colored crystalline solid was separated and characterized. IR (KBr disk cm-1): 3352, 1616, 1568, 1392, 923, 733, 659 cm–1. 3482 (OH), 3409 (-NH2), 3311 (-NH-), 2971

(CHAr), 1647 (-CO), 1585 (-N=CH-), 1132 (-C-C-C-), 1078 (CHAr).

Synthesis of [Cu(SalArgH)]$NO_3 \cdot H_2O$ (CuAr)

The procedure mentioned above was followed, and the volume of the Schiff base was reduced by 2/3. Subsequently, 10 ml of an aqueous solution of $Cu(NO_3)_2 \cdot H_2O$ (1.208 g, 5 mmol) was added, changing the color from yellow to dark green. The resulting clear solution was left for crystallization at room temperature. About 15 days later, we obtained green-colored, flake-shaped, single crystals used for single-crystal diffraction. yield 1.40 g (3.34 mmol, 68%). IR (KBr disk cm-1): 3345, 3183, 2948, 2866, 1634, 1634, 1440, 1317, 1243, 1269, 1194, 1194, 1162 1006, 751, cm–1. C13H18CuN5O7 (419.86): calcd. C 12.01, H 1.01, N 14.01; found C 12.18, H 1.61, N 13.78.

X-ray crystallography

Data for CuAr was collected on a Bruker Smart Apex CCD X-ray diffractometer using graphite monochromated Mo-Kα radiation. The data were reduced using SAINTPLUS,[15], and multiscan absorption corrections using SADABS[16] were applied. The structures were solved using SHELXS-97[17] and refined using SHELXL-2018.[17] All ring hydrogen atoms were assigned based on geometrical considerations and were allowed to ride upon the respective carbon atoms.

Crystal Structure

Single-crystal analysis showed the 1D coordination polymer [Cu(SalArgH)]$NO_3 \cdot H_2O$ (CuAr) crystallizes in an orthorhombic crystal system having $P2_12_12_1$ space group, and asymmetric unit (Figure 1a) of one protonated ligand unit, one copper atom, one lattice water molecule, and one nitrate anion for balancing the overall charge. The ligand acts as a tridented chelating ligand [Fig. 1a], as many reported salicylic acid and amino acids-based Schiff bases. [18-22] The other two coordination sites of square pyramidal Cu-atoms are occupied by crystallographically two different carboxylates (O2, -C-O-) and carboxyl (O3, -C=O) oxygen atoms respectively. Therefore, the ligand SalArg simultaneously bridges two neighbouring Cu^{2+} ions and forms an isosceles triangle (Fig. 1b) with the side lengths *viz*. 3.598, 3.598, and 4.958 Å. Furthermore, from the crystal structure, it was revealed that the complex is a one-dimensional coordination polymer (Figure 1c) with square pyramidal -$O2^{i}$-Cu(SalArg)-$O3^{ii}$- building blocks [Fig. 1a]. The side chains of the arginine molecule help to adopt a helical 1D coordination polymer (Fig. 1c). The coordination polymer propagates along the crystallographic *a*-axis, forming a right-handed (P) helical chain supported by bridging carboxylate coordination of the Schiff base ligand (Fig. 1d). Besides that, the tail of the L-arginine, *i.e*. -NH-C(-NH_2)(=NH_2^+), forms 1D H-bonded networks with nitrate anion (Fig. 1e and Fig 1f representing the packing diagram supported by the H-bonds, stabilized the overall helical nature of the polymer). Selected bond lengths and angles, and all H-bonding interactions are listed in Table 2 and Table 3, respectively. Also observed that the τ parameter calculated using the two largest gest coordination angles (β = 170.3° and α = 167.1°) is 0.05, indicating that the Cu(II) center adopts an almost ideal square pyramidal geometry with negligible distortion toward a trigonal bipyramidal geometry.

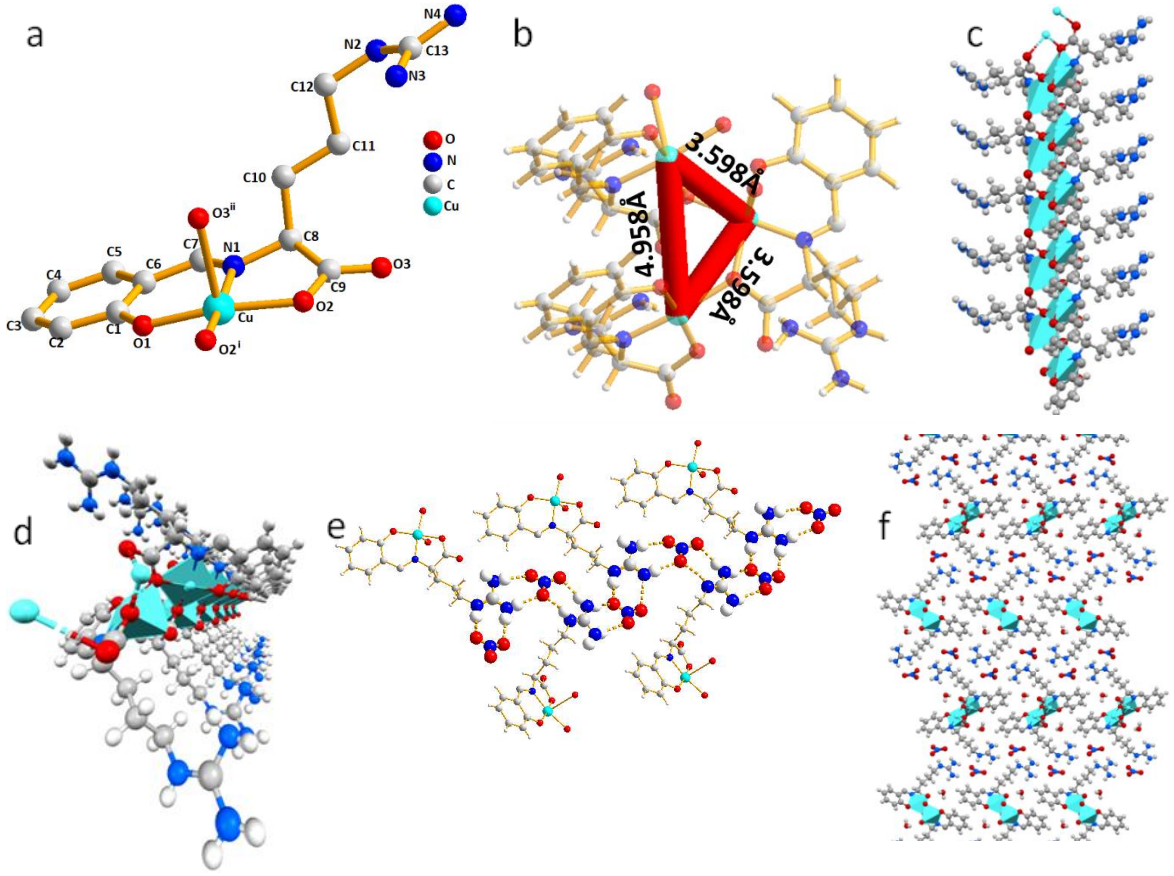


Figure 1. (a) Coordination environment around Cu^{2+} ion in a monomer unit, (b) isosceles triangle formed by three neighbouring Cu^{2+} ion, (c) one single 1D polymeric chain with pentagonal polyhedral possessed by Cu^{2+} ion, (d) perspective view to visualize the helical structure of the 1D coordination polymer propagating through *a*- axis, (e) hydrogen-bonded loop between -NH-C(-NH_2)(=NH_2^+) tail and NO_3^- ion, (f) packing diagram along the *a* axis.

Table 1. Crystal data and structure refinement parameters for **CuAr**

Compound	**CuAr**
Empirical formula	$C_{13}H_{18}CuN_5O_7$
Formula weight	419.86
Temperature (K)	293(2)
Wavelength(λ)	0.71073 A
Crystal system	Orthorhombic
Space group	$P2_12_12_1$
a[Å]	4.9577(11)
b[Å]	11.7724(17) A
c[Å]	29.154(4)
α[°]	90
β[°]	90
γ[°]	90
Volume[Å^3]	1701.6(5)
Z	4
Density (calculated) [Mg/m^3]	1.639
Absorption coefficient [mm^{-1}]	1.332
F(000)	864
Refl. used [$I > 2\sigma(I)$]	3480
Independent reflections	5264
R_{int}	0.0572
Refinement method	Full-matrix least-squares on F^2
GOF	1.014
Final *R* indices [I>2σ(I)][a]	0.0637
R indices (all data)[b]	0.1060
2θ	2.795 to 29.021
CCDC No	1904735

[a] $R1 = \Sigma||F_o|-|F_c||/\Sigma|F_o|$, [b] $_wR2 = \{\Sigma_w[(|F_o|^2 - F_c|^2)]^2/\Sigma|_w(F_o^2)|^2\}^{½}$

Table 2. Selected bond distances (Å) and bond angles (º) for (**CuAr**)			
O2-Cu1	1.987(4)	Cu1-N1	1.902(6)
Cu1-O1	1.889(5)	Cu-O3#2	2.595(5)
Cu1-O2#1	2.000(5)	N1-Cu1-O2#1	170.3(2)
O1-Cu1-O2	89.5(2)	O1-Cu1-O2#1	89.5(2)
O2-Cu1-O2#1	94.9(2)	O3-Cu1-O2#1	77.0(2)
O3#2-Cu1-O2	93.2(2)	O3-Cu1-O1	97.5(2)
O1-Cu1-N1	94.6(2)	O2-Cu1-N1	82.5(2)
O1-Cu1-O3#2	97.5(2)	O2-Cu1-O3	93.2(2)
O2-Cu1-O2	94.9(2)	O3#2-Cu1-N1	93.8(2)
O2-Cu1-O1	167.1(2)	O3-Cu1-O2#1	77.0(2)

#1 *x*-1/2, -*y*+3/2, -*z*, #2 1/2-x, -*y*,3/2+*z*

Table 3. All possible Hydrogen bonded contact

D-H···A	d(D-H)(Å)	d(A···H)(Å)	<(DHA) (°)
N2-H2A···O5	0.83(9)	2.10(9)	146.94
N3-H3A···O1w	0.82(6)	2.41(7)	148.61
N3-H3B···O4	0.83(6)	2.05(5)	146.71
N4-H4A···O6	0.85(7)	2.11(7)	174.29
O1w-H1wA···O3	0.83(7)	2.28(8)	156.30
O1w-H1wB···O1	0.84(5)	2.21(5)	164.84

Hirshfeld surface analysis for CuAr

Hirshfeld surface (HS) analysis and the associated two-dimensional (2D) fingerprint (FP) plots were generated using *CrystalExplorer* 3.0.62 to investigate the intermolecular interactions governing the crystal packing of CuAr. [23-24] This approach provides an effective framework for visualizing and correlating intermolecular contacts with the resulting supramolecular architecture. [14,23-24,28]. The Hirshfeld surface is defined as the region in a crystal where the electron density contribution from a molecule equals that from the surrounding crystal environment, *i.e*., where the promolecule-to-procrystal electron density ratio is 0.5.[14, 24–26,28,30] Consequently, the shape and features of the HS are highly sensitive to the molecular environment within the crystal. For each point on the Hirshfeld surface, two distances are considered: d_i (distance to the nearest internal nucleus) and d_e (distance to the nearest external nucleus). These parameters combine to yield the normalized contact distance d_{norm}, which highlights intermolecular interactions. On the d_{norm} surface, red, white, and blue regions correspond to contacts shorter than, equal to, or longer than the sum of van der Waals radii, respectively. [14, 23–26,28,30] In this study, HS analysis was performed at both molecular and atomic levels. For molecular-level analysis, the asymmetric unit excluding lattice water molecules and nitrate ions was considered, thereby focusing on intrinsic ligand–metal interactions. The three-dimensional HS mapped over d_{norm}, along with shape index (S) and curvedness (C), and the corresponding 2D FP plots, are presented in Fig. 2 and 3. Standard surface resolution and appropriate transparency settings were employed to ensure clear visualization of intermolecular contacts.

To further probe the influence of coordination on HS properties, atomic-level HS analysis was carried out (Fig. S4). This approach

enables examination of subtle surface features such as depressions, which are sensitive to ligand characteristics and significantly influence HS parameters, including volume, globularity, and asphericity.[14, 25, 30] Unlike molecular HS analysis, this method provides deeper insight into atom-specific contributions to intermolecular interactions.

The HS mapped over d_{norm} reveals prominent interaction features. Intense red spots around oxygen atoms indicate strong O···H intermolecular contacts arising from hydrogen bonding involving ligand carboxyl oxygen atoms and lattice water molecules. These contacts are quantitatively supported by FP plots (Fig. 3), where O···H/H···O interactions contribute 27.4% and appear as sharp spikes at low d_e+d_i values (< 2.5 Å), consistent with strong hydrogen bonding interactions reported in Hirshfeld-based analyses.[14,24–25,28,30] Experimental hydrogen bond distances (~2.05 Å and ~2.41 Å) further confirm their strength and directionality. Additionally, blue depressions around the ligand side chain are attributed to H···O interactions involving the –NH–C(–NH_2)(=NH_2^+) moiety and nitrate ions, reflecting reduced d_e and d_i values and resulting in negative d_{norm}. In contrast, N···H interactions contribute ~6.9% and appear as smaller spikes at higher d_e+d_i values (~2.7–2.9 Å), indicating weaker interaction strength compared to O···H contacts, consistent with earlier HS studies.[14,25,28] Similarly, C···H/H···C interactions contribute 12.6% and manifest as broad, diffuse regions in FP plots, corresponding to near-zero or slightly positive d_{norm}, characteristic of weak van der Waals interactions. [14,25,28] These interactions play a secondary role in stabilization and packing efficiency rather than directing the primary structure. Although Cu–O and Cu–N bond lengths define the primary coordination geometry around the Cu(II) center (Fig. 1), their contribution to supramolecular assembly is indirect. The Cu–O bonds enhance electron density localization on oxygen donor atoms, strengthening their ability to act as hydrogen bond acceptors, which is clearly reflected in the HS features and FP contributions.[14,23-24,28] A similar but weaker effect is observed for nitrogen donor atoms. Importantly, the absence of short Cu···Cu or significant Cu···O intermolecular contacts, along with their negligible FP contributions, suggests that the coordination sphere is electronically saturated and does not actively participate in secondary intermolecular interactions, consistent with related coordination systems.[25,27,30] Additional insights are obtained from the shape index and curvedness surfaces (Fig. 2). The absence of complementary red–blue triangular patterns in the shape index confirms the lack of π···π stacking interactions, while curvedness plots show predominantly flat regions, indicating localized rather than extended planar interactions.[14, 24-26, 28] This explains the formation of a one-dimensional helical arrangement instead of layered packing. From a structure–interaction perspective, a clear relationship emerges: Cu–O coordination enhances electron density on oxygen, leading to strong O···H hydrogen bonding, lower d_e and d_i, more negative d_{norm}, and the highest FP contribution (27.4%), whereas Cu–N coordination results in weaker N···H interactions with lower FP contributions (~6.9%).

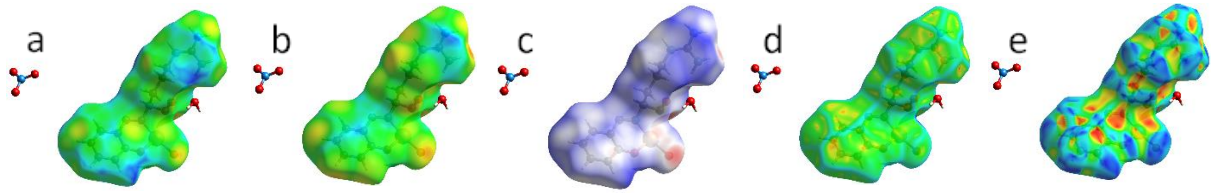
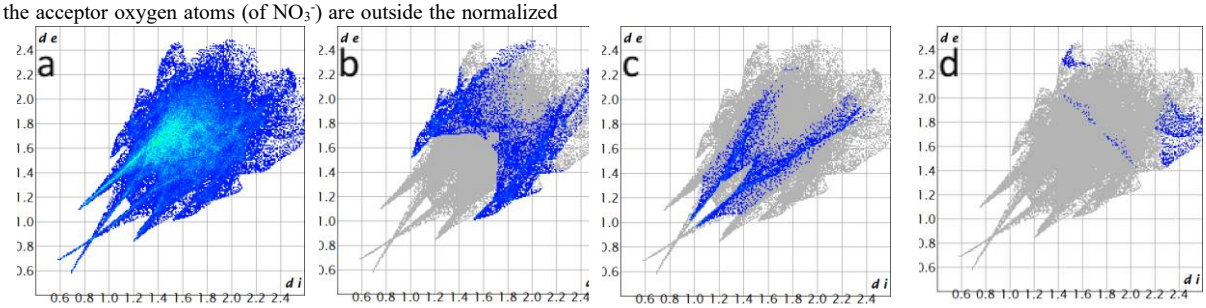


Figure 2. Hirshfeld surface representations and their ranges in parathesis (a) d_e (0.9240 to 2.2202Å) (b) d_i (0.9660 to 2.9119Å) (c) d_{norm} (-0.7045(red) to 1.7758 Å(blue) Å) (d) shape index (-1.0000 to 1.0000Å) (e) curvedness (-4.0000 to 0.4000Å).

The 2D fingerprint maps of CuAr provide quantitative information on the individual contribution of intermolecular interactions in the symmetric unit (see Figure 3). In the asymmetric unit, the most abundant intermolecular interactions are C···H (12.6%), Cu···O (6.2%), Cu···H (1%), O···H (27.4%), and N···H (6.9%). The de (y-axis) and di (x-axis) represent the nearest internal and external distances (in Å) using points on the Hirshfeld surface contact. This structure contains two types of hydrogen bonds: (i) a 1D loop between the NO_3^- ion and arginine tail (see Figure 1e and Table 3), and (ii) between lattice water and ligand's oxygen atoms (O1 and O3, Table 3). In the first case, the ligand N atoms act as donor atoms and are located inside, while the acceptor oxygen atoms (of NO_3^-) are outside the normalized surface of the asymmetric unit, contributing to 20.7% of the overall interactions. In the second case, the donor water molecules are inside, while the acceptor oxygen atoms (of the ligand) are outside the normalized surface, contributing 6.7%, which is comparatively less than in the previous case. The $O\cdots H_{reciprocal}$ represents a distinct upper donor lower acceptor spike, representing O···H/H···O contacts around $d_e + d_i < 2.5$ Å. The 2D FP representation of N···H/H···N shows a similar contribution, 3.5% and 3.4% respectively, with $d_e + d_i \sim 2.8$ Å. Other than minor Cu···H/H···Cu (1%) contacts, no significant Cu···C, Cu···N, Cu-Cu, and O···N intermolecular contacts are found in FP plots.



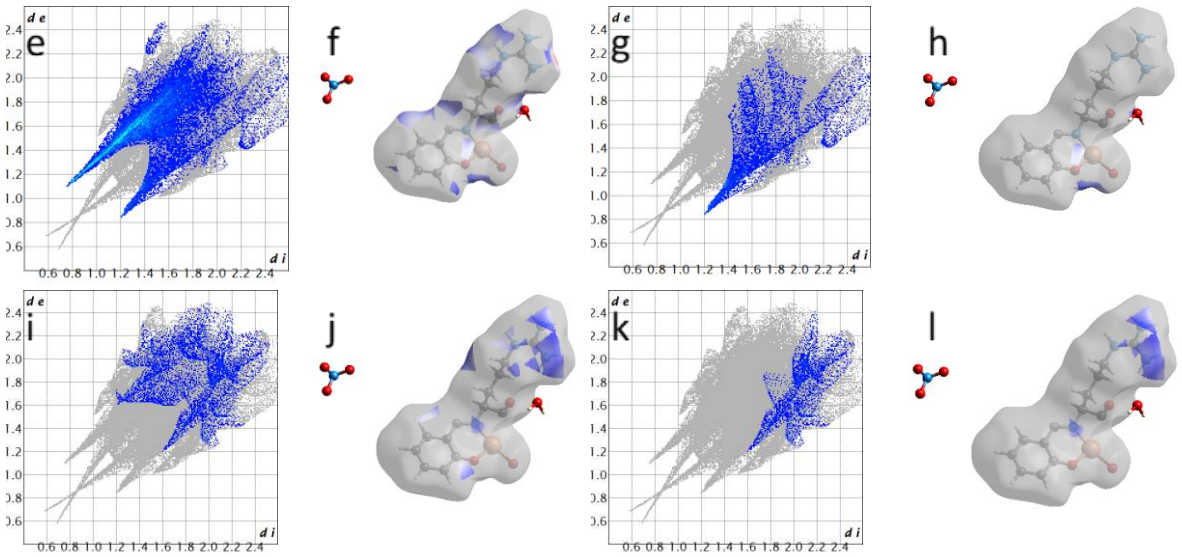


Figure 3. (a) all interactions (b) C···$H_{reciprocal}$ (12.6%) (c) Cu···$O_{reciprocal}$ (6.2%) (d) Cu···$H_{reciprocal}$ (1%) (e) O···$H_{reciprocal}$ (27.4%) (f) d_{norm} surface concerning O···$H_{reciprocal}$ (g) O_{ins}···H_{outs} (6.7%)(h) d_{norm} surface concerning O_{ins}···H_{outs} (i) N···$H_{reciprocal}$ (6.9%) (J) d_{norm} surface concerning N···$H_{reciprocal}$ (k) N_{ins}···H_{outs} (3.4%) (l) d_{norm} surface concerning N_{ins}···H_{outs}.

From a geometrical standpoint, the Hirshfeld volume (V_H) and surface area (A_H) indicate compact molecular packing, while globularity (G < 1) and moderate asphericity (Ω) suggest a slightly anisotropic yet well-defined molecular surface. [14,25,30] Notably, the HS around the Cu(II) center exhibits higher globularity and lower asphericity compared to the overall molecule, indicating a more symmetric local coordination environment. This contrast between local symmetry and global anisotropy further confirms that intermolecular interactions are primarily governed by ligand functionalities rather than coordination geometry. [14,25,30]

Table 3. Quantitative data from molecular and atomic Hirshfeld surface analyses of **CuAr**

Optimization	V_H(Å^3)	A_H(Å^2)	G	Ω
$HS_{Cu\text{-}SalArg}$	336.46	333.09	0.702	0.355
HS_{Cu}	14.19	33.89	0.836	0.151

Electronic Spectra and Circular Dichroism

The UV–Vis and CD spectra of the Cu(II)-coordinated arginine–salicylaldehyde Schiff base polymer provide complementary but fundamentally different information about the system. The UV–Vis spectrum (Fig.4a) mainly shows electronic absorption processes, with a band at higher energy (280nm) attributed to π-π* transitions of the phenyl ring, while the stronger, lower- energy band at 300-350 nm is assigned to n- π* transition of the azomethine (–CH = N–) group. The electronic absorption and chiroptical properties of the Cu(II)-coordinated arginine–salicylaldehyde Schiff base polymers are inherently related, with the UV–Vis and CD spectra (Fig. 4b) together revealing both electronic structure and supramolecular organization. The splitting and broadening seen in the UV–Vis spectrum result from tetragonal pyramidal coordination around the Cu(II) center, which lifts the degeneracy of the d- orbitals and produces multiple d–d transitions, further intensified by strong Jahn–Teller distortion typical of the d^9 configuration. [31–33] Additionally, overlapping ligand- to- metal charge transfer (LMCT) transitions and reduced symmetry contribute to the structured absorption profile.[31, 34] Notably, these electronically split transitions form the foundation for the bisignate Cotton effects observed in the CD spectrum, where the π → π* bands in the 200–250 nm region show clear exciton splitting due to coupling between spatially arranged chromophores along the helical polymer backbone. [35-36] Therefore, while the UV–Vis spectral splitting originates from ligand field effects and metal–ligand electronic interactions, the corresponding CD splitting results from exciton coupling between these electronically active units within a chiral environment. The additional CD activity seen in the LMCT region (320–360 nm) further confirms that the Cu(II) centers themselves take part in the chiral organization, showing that the helical structure propagates through both ligand framework and metal coordination sites.[35] This direct link between UV–Vis band splitting and CD exciton coupling strongly supports the idea of a one- dimensional helical coordination polymer with effective chirality transfer and amplification from the arginine ligand to the metal- organized framework.

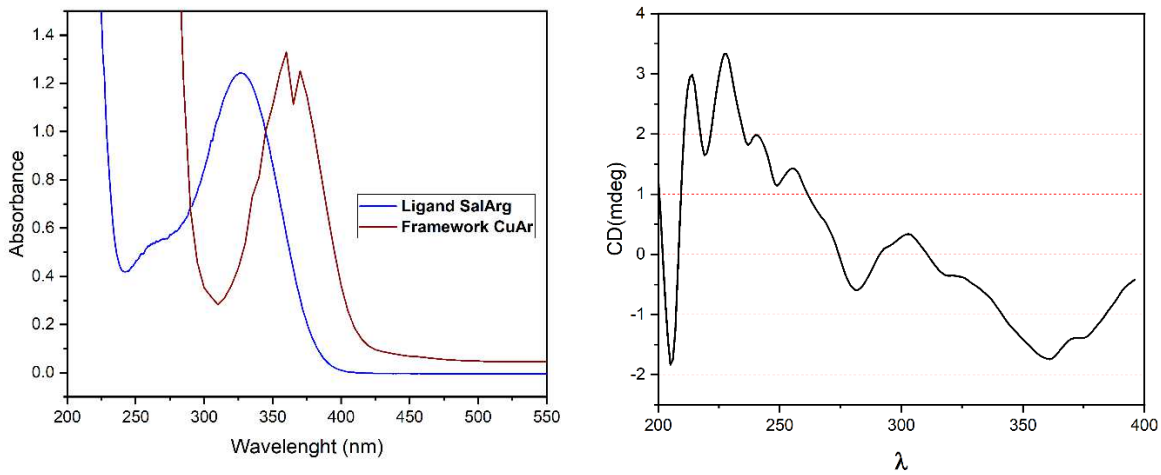


Figure 4. (a)Electronic spectra of ligand $SalArgH_2$ and complex (CuAr) (b) circular dichroism of complex.

Conclusions

In summary, a new chiral one-dimensional Cu(II) coordination polymer, based on an L-arginine Schiff base, has been successfully synthesized and structurally analyzed. Single-crystal X-ray analysis shows that the tridentate ligand links neighboring Cu(II) centers, forming a helical polymer chain with a distorted square pyramidal coordination geometry. The inherent chirality of the L-arginine moiety is effectively transferred to the extended coordination framework, resulting in a well-defined helical structure. Hirshfeld surface analysis indicates that directional O···H hydrogen-bonding interactions are key to stabilizing the supramolecular architecture and maintaining the helical shape. Spectroscopic studies support the structure–property relationship: UV–Vis spectra reveal ligand-field splitting and Jahn–Teller distortion, while circular dichroism (CD) spectra show characteristic bisignate Cotton effects from exciton coupling between chromophores aligned along the helical backbone. These results clearly demonstrate the transfer of chirality from the molecular to the supramolecular level. Overall, this work highlights how amino acid-derived Schiff base ligands can guide helical assembly and enable effective chirality transfer in coordination polymers. The combined structural, Hirshfeld surface, and chiroptical analyses provide valuable insights for the rational design of chiral functional materials with potential applications in optics, sensing, and biomimetic systems.

Supplementary Information

The online version contains supplementary material available

Acknowledgments SME thanks the Department of Chemistry Instrumentation Facilities, IIEST Shibpur, for the spectral and analytical data, and the School of Chemistry, the University of Hyderabad, for the X-ray data collection.

Declarations:

The author declares no conflict of interest

Funding: Not applicable

Data Availability Statement: CCDC 1904735, the supplementary crystallographic data for CuAr. These data can be obtained free of charge via www.ccdc.cam.ac.uk, or from the Cambridge Crystallographic Data Centre, 12 Union Road, Cambridge CB2 1EZ, UK; fax: (+44) 1223-336-033; or e-mail: deposit@ccdc.cam.ac.uk.

References

1. Kumari N, Singh RK, Kumar P (2022) Transition metal complexes of amino acid Schiff bases: synthesis, characterization and applications. J Mol Struct 1245:131234
2. Abdel-Rahman LH, Abu-Dief AM, Ismael M, Mohamed AA (2013) Synthesis, characterization and antimicrobial activity of metal complexes with Schiff base ligands. J Chem Pharm Res 5:176–184
3. Subha L, Mahalakshmi R, Raman N (2015) DNA binding, cleavage and anticancer studies of Schiff base metal complexes. Spectrochim Acta A Mol Biomol Spectrosc 137:140–149
4. Wazalwar SS, Rao CP, Rao G (2012) Antioxidant activity of transition metal Schiff base complexes. J Chem Sci 124:639–647
5. Fan Y, Zhang Y, Liu H (2024) Role of L-arginine in cardiovascular health and metabolic regulation. Nutrients 16:1123
6. Wojciechowska A, Muzioł T, Lewiński K (2015) Coordination behavior of amino acid-derived ligands in metal complexes. Polyhedron 102:425–432.
7. Raman N, Kulandaisamy A, Thangaraja C (2004) DNA interaction, antimicrobial and electrochemical studies of transition metal(II) complexes with Schiff base ligands. J Chem Sci 116:209–213.
8. Kovala-Demertzi D, Demertzis MA, Miller JR, Frampton CS, Jasinski JP, West DX (2006) Platinum(II) complexes of Schiff bases: synthesis, structure and biological activity. Polyhedron 25:117–124.
9. Sasmal PK, Majumdar R, Dighe RR, Chakravarty AR (2010) Photocytotoxicity and DNA cleavage activity of L-arginine and L-lysine Schiff base oxovanadium(IV) complexes. Dalton Trans 39:7104–7113.
10. Kołodziej B, Kochel A, Woźniak K (2014) Salicylaldehyde–arginine Schiff base: synthesis and structural characterization. Inorg Chim Acta 423:136–142
11. Zhang Y, Li B, Ma H, Wang L (2017) Schiff base-based coordination polymers: synthesis, structures and properties. CrystEngComm 19:3215–3223
12. Li X, Wu Y, Chen Z, Zhang J (2019) Construction of transition metal coordination polymers from Schiff base ligands. Dalton Trans 48:12345–12353
13. Wang J, Liu Q, Zhao H, Sun W (2020) Structural diversity of Schiff base coordination polymers and

their functional properties. Inorg Chem Front 7:210–220
14. Spackman MA, Jayatilaka D (2009) Hirshfeld surface analysis. CrystEngComm 11:19–32.
15. Bruker AXS Inc. (2003) SAINTPLUS. Bruker AXS Inc., Madison, WI, USA
16. Sheldrick GM (1996) SADABS: Program for empirical absorption correction. University of Göttingen, Göttingen, Germany
17. Sheldrick GM (1997) SHELX-97: Programs for crystal structure analysis—University of Göttingen, Göttingen, Germany.
18. Kumari S, Yadav P, Sharma S, Ranka M (2022) Amino acid based Schiff bases and their metal complexes as biologically potent agents. Asian J Chem 34:2465–2477
19. Abdel-Rahman LH, Abu-Dief AM, El-Khatib RM, Abdel-Fatah SM (2016) Some new nano-sized Fe(II), Cd(II) and Zn(II) Schiff base complexes: synthesis, characterization and biological studies. J Mol Struct 1103:232–244
20. Mohamed GG, Omar MM, Ibrahim AA (2021) Synthesis, spectroscopic and biological studies of metal complexes with Schiff base ligand derived from salicylaldehyde. Z Anorg Allg Chem 647:1685–1693.
21. Mahadevi P, Shanmugam S (2024) Synthesis, characterization, and biological activity of transition metal complexes with Schiff base ligands. Results Chem 6:101234.
22. Gupta KC, Sutar AK (2008) Catalytic activities of Schiff base transition metal complexes. Coord Chem Rev 252:1420–1450.
23. McKinnon JJ, Spackman MA, Mitchell AS (2004) Novel tools for visualizing intermolecular interactions in molecular crystals. Acta Crystallogr B 60:627–668.
24. Spackman MA, McKinnon JJ (2002) Fingerprinting intermolecular interactions in molecular crystals. CrystEngComm 4:378–392.
25. Spackman MA (2013) Hirshfeld surface analysis: a practical tool for crystal engineering. Phys Scr 87:048103.
26. Turner MJ, McKinnon JJ, Wolff SK et al (2017) CrystalExplorer17. University of Western Australia.
27. Spackman PR, Turner MJ, McKinnon JJ et al (2021) CrystalExplorer: a program for Hirshfeld surface analysis. J Appl Crystallogr 54:1006–1011.
28. McKinnon JJ, Jayatilaka D, Spackman MA (2007) Towards quantitative analysis of intermolecular interactions. Chem Commun:3814–3816.
29. Hirshfeld FL (1977) Bonded-atom fragments for describing molecular charge densities. Theor Chim Acta 44:129–138.
30. Spackman MA, McKinnon JJ, Jayatilaka D (2008) Electrostatic potentials mapped on Hirshfeld surfaces. CrystEngComm 10:377–388.
31. Elmali A, Elerman Y (2022) Spectroscopic and structural characterization of copper(II) Schiff base complexes. Spectrochim Acta A 264:120265
32. Kumar S, Dhar DN, Saxena PN (2023) Applications of metal complexes of Schiff bases—A review. Coord Chem Rev 475:214890
33. Zhang D et al. (2024) Chiral self-assembly of coordination polymers with amplified circular dichroism. Nat Commun 15:4685
34. Yang Y et al. (2023) Exciton-coupled circular dichroism in supramolecular helical systems. Chem Sci 14:11234–11242
35. Pescitelli G, Di Bari L (2023) Applications of electronic circular dichroism in coordination chemistry. Coord Chem Rev 470:214710
36. Liu M, Zhang L, Wang T (2022) Supramolecular chirality in self-assembled systems. Nat Rev Chem 6:162–176.

Supplementary Files

This is a list of supplementary files associated with this preprint. Click to download.

- SupportinginformationCuSalarg.docx